ACS APPLIED MATERIALS & INTERFACES

Research Article

www.acsami.org

Boosting Performance of Low Temperature Fuel Cell Catalysts by Subtle Ionic Liquid Modification

Gui-Rong Zhang, Macarena Munoz, and Bastian J. M. Etzold*

Lehrstuhl für Chemische Reaktionstechnik Friedrich-Alexander-Universität Erlangen-Nürnberg (FAU), 91058 Erlangen, Germany

Supporting Information

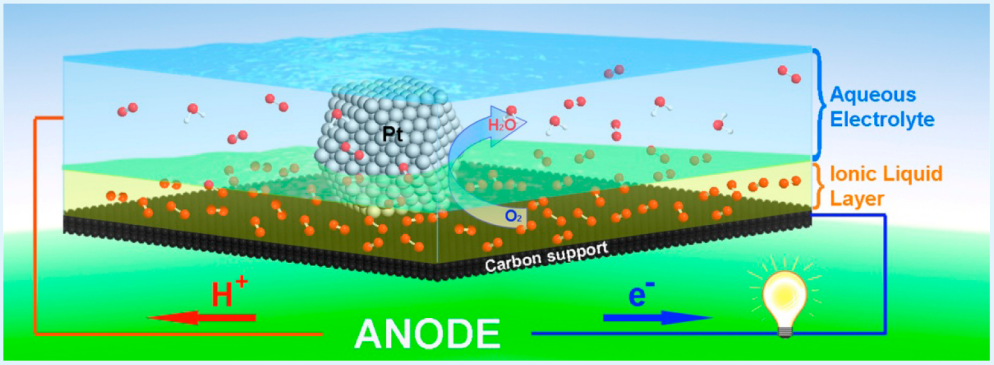

ABSTRACT: High cost and poor stability of the oxygen reduction reaction (ORR) electrocatalysts are the major barriers for broad-based application of polymer electrolyte membrane fuel cells. Here we report a facile and scalable approach to improve Pt/C catalysts for ORR, by modification with small amounts of hydrophobic ionic liquid (IL). The ORR performance of these IL-modified catalysts can be readily manipulated by varying the degree of IL filling, leading to a 3.4 times increase in activity. Besides, the IL-modified catalysts exhibit substantially enhanced stability relative to Pt/C. The enhanced performance is attributed to the optimized microenvironment at the interface of Pt and electrolyte, where advantages stemming from an increased number of free sites, higher oxygen concentration in the IL and electrostatic stabilization of the nanoparticles develop fully, at the same time that the drawback of mass transfer limitation remains suppressed. These findings open a new avenue for catalyst optimization for next-generation fuel cells.

KEYWORDS: *oxygen reduction, supported Pt catalysts, ionic liquids, SCILL, mass transfer*

INTRODUCTION

Polymer electrolyte membrane fuel cells (PEMFCs) featuring low operating temperature, high power density, and easy scale-up, are considered as key technology for the next generation of power sources for transportation, stationary and portable applications.[1−3] However, the high cost and poor stability of the state-of-the-art Pt/C catalyst, which is an indispensable component to facilitate both anodic and cathodic reactions,[4,5] remain as tremendous challenges for the broad-based applications of PEMFC technologies. The sluggish kinetics of the cathodic oxygen reduction reaction (ORR) and the demands of the complex 4-electron ORR pathway pose major barriers to reduce the Pt loading. Besides, degradation of the electrocatalyst caused, e.g., by poisoning, particle detachment, agglomeration and/or carbon corrosion also needs to be tackled to obtain reliable systems.[6]

In the past decade, intense research efforts have been devoted to improve the catalytic performance for ORR by engineering the active site, e.g., in size, shape and composition. For instance, tuning the electronic properties of Pt with bi- or multimetallic nanostructures has been proven effective to increase the intrinsic activity and long-term stability of Pt.[1,2,4,6−10] Stamenkovic et al. reported that a $Pt_3Ni(111)$ alloy surface showed 10-fold higher activity for the ORR than the corresponding Pt(111) surface and 90-fold higher than the commercial Pt/C catalyst.[2] Most recently, Chen et al. reported that Pt_3Ni nanoframe catalysts with edge width of 2 nm achieved 22-fold enhancement in specific activity relative to Pt/C for ORR.[11] Regarding the stability issue, Adzic et al. demonstrated that Pt fuel-cell electrocatalysts can be stabilized against dissolution by combining Pt nanoparticles with gold (Au) clusters.[2] Moreover, Popov et al. found that the presence of Ni in Pt_3Ni/C catalysts could efficiently prevent the active Pt particles from coalescence.[12] Although these approaches demonstrated significant potential, the complex synthetic procedures involved and the higher effort in recycling of mixed metal catalysts causes some economic concerns.

Apart from tuning the active sites, it is also recognized that the solid (Pt)−liquid (electrolyte) interface plays a major role in the ORR.[13−15] Hence, manipulation of this interface offers

Received: October 24, 2014
Accepted: January 26, 2015
Published: January 26, 2015

DOI: 10.1021/am5074003
ACS Appl. Mater. Interfaces 2015, 7, 3562−3570

an alternative to optimize the catalyst performance. We here present an approach to modifying the surface of a conventional Pt/C catalyst with small amounts of hydrophobic ionic liquid (IL), creating a novel solid−liquid−liquid microenvironment of Pt, IL and aqueous electrolyte. A similar concept was applied to heterogeneous catalysts as early as 2007 and the term "SCILL" (Supported Catalysts with Ionic Liquid Layer) was coined for this kind of catalyst treatment and modification.[16] This was demonstrated first for the selective Ni-catalyzed hydrogenation of dienes by some authors of this paper and later studied in other reactions (e.g., hydrogenation of citral, limonene and acetylene, and skeleton isomerization of *n*-octane) from an applied and fundamental point of view.[16−20] The significant activity and selectivity improvements resulting from ionic liquid coating of traditional heterogeneous catalysts have been shown to origin from a combination of local changes in concentration at the active sites (due to differential solubility properties of the IL) and changes in the electronic environment by direct ligand effects or coadsorption. Nevertheless, to the best of our knowledge, the SCILL concept has not been intentionally applied to electrocatalytic systems despite the fact that ILs have already been widely used in electrochemistry due to their good ionic conductivities, wide electrochemical windows, and suitable thermal/chemical stabilities.[21−25] Recently, electrocatalyst composites with some similarity to the SCILL concept (the catalyst being completely filled with IL) were introduced. Unsupported and carbon supported porous PtNi nanoparticles, prepared by electrochemical etching, were impregnated with the IL $[MTBD][N(SO_2C_2F_5)_2]$ (Scheme S2, Supporting Information) and tested in ORR using an aqueous electrolyte.[26,27] A 2 to 3 times higher intrinsic activity of these composite electrocatalysts was observed compared to the PtNi catalysts without IL. However, the tedious synthetic approach to the porous PtNi NPs, involving various organic reducing/capping agents, solvothermal process and electrochemical etching treatment, is rather limited in terms of production volume. Similarly, Zheng et al. fabricated a Pt-IL composite catalyst by impregnating graphene supported Pt nanoparticles with a similar IL ($[MTBD][NTf_2]$) (Scheme S2, Supporting Information), and found that the composite electrocatalysts exhibited enhanced intrinsic activity for ORR and higher methanol tolerance relative to its counterpart without IL.[28] Nevertheless, the Pt-IL composites were obtained by placing a drop of IL onto the Pt catalyst modified electrode, which made it difficult to achieve large batch production and showed little controllability over microenvironment of Pt, IL and aqueous electrolyte. These initial reports demonstrate the great potential of IL modification for boosting activity of noncommercial Pt on carbon electrocatalysts for ORR, while it is still highly desirable to develop facile and scalable approach to synthesizing SCILL-concept based electrocatalysts and to comprehensively understand the behavior of IL in these IL-modified catalytic systems.

Herein, the SCILL concept in electrocatalysis is studied in detail by impregnating varying amounts of IL ($[MTBD][NTf_2]$) into the pores of a Pt/C catalyst, enabling us to systematically tune the microenvironment of the solid−liquid−liquid interfaces (Scheme 1). We report the surprising fact that both, the ORR activity and the stability of the IL modified Pt/C catalysts (denoted as Pt/C-SCILL-α, α: pore filling degree) can be readily manipulated by varying the degree of IL filling. A partial IL filling has been identified as optimal. Remarkably, the Pt/C-SCILL with 50% pore filling possesses a mass activity of 0.56 A mg^{-1}_{Pt} at 0.9 V, which is substantially higher than the mass activity target (0.44 A mg^{-1}_{Pt}) set by the US Department of Energy for 2017−2020. These findings demonstrate for the first time that a high-performing ORR catalyst can be produced by modifying a commercial catalyst in a facile modification protocol using small amounts of IL. These findings demonstrate a great potential of the SCILL concept to improve the activity and stability of Pt catalysts for the cathode reaction.

Scheme 1. Schematic Illustration of the SCILL Concept for Cathodic ORR on a Pt/C Material[a]

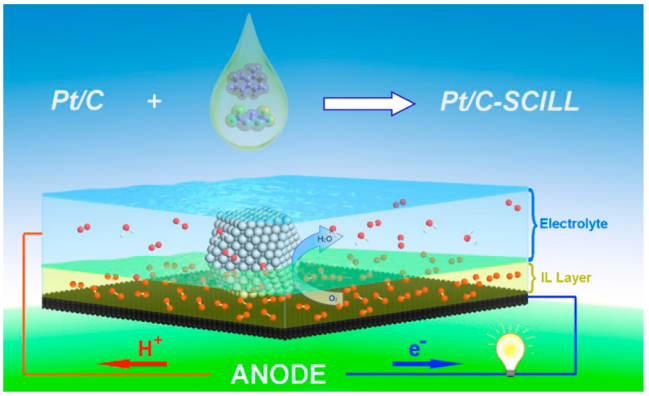

[a]On the carbon support surface, a hydrophobic IL-layer is deposited and in direct contact to the aqueous electrolyte, supplying oxygen for the reaction. Depending on the IL-layer thickness, the platinum nanoparticle is partially or fully covered.

EXPERIMENTAL SECTION

Reagents. Pt/C catalyst (20 wt %, HiSPEC-3000, Jonhson Matthey) was purchased from Alfa Aesar and used as a benchmark and reference catalyst for ORR measurements. $HClO_4$ solution (70%) and 7-methyl-1,5,7-triazabicyclo[4.4.0]dec-5-ene ([MTBD]) (98%) were purchased from Sigma-Aldrich. Lithium bis(trifluoromethylsulfonyl)imide ($[NTf_2]$) (99%) was from IoLiTec GmbH. All the chemicals were used as received without further purification. Deionized water was used in all of the preparations.

Synthesis of $[MTBD][NTf_2]$ IL. The $[MTBD][NTf_2]$ IL was synthesized following a literature procedure.[28] Briefly, equimolar amounts of the precursors 7-methyl-1,5,7-triazabicyclo[4.4.0] dec-5-ene [MTBD] (5.2 g, 33.9 mmol) and the lithium salt of bis(trifluoromethylsulfonyl)imide $[NTf_2]$ (9.7 g, 33.9 mmol) dissolved in water with HNO_3 were cooled in ice near 0 °C. HNO_3 was added dropwise to the [MTBD] solution until neutral pH was reached. Then, the $Li[NTf_2]$ solution was slowly added and the IL precipitated as a viscous fluid phase beneath the water phase. The IL was washed several times with ultrapure water and then placed in a rotary evaporator (Büchi Rotavapor R-220) at 60 °C for 24 h to remove residual water. The IL was further dried under high vacuum. Karl Fischer titration showed water content of the IL below 200 ppm. The high purity of the as-prepared IL was verified by the NMR spectra (Figure S1, Supporting Information).

Synthesis of Pt/C-SCILL System. The SCILL systems were synthesized by coating commercial Pt/C catalyst with the as-prepared $[MTBD][NTf_2]$. A typical synthesis procedure for a SCILL system is as follows: 90 mg of Pt/C (JM) catalyst was mixed with 10 mL of isopropyl alcohol solution containing a specific amount of IL under intense stirring at room temperature. After 20 min ultrasonic treatment of this mixture, the volatile solvent isopropyl alcohol was slowly removed from the slurry by rotary evaporation under low vacuum (137 mbar, 60 °C) and followed by further evaporation at 8 mbar vacuum to ensure complete intrusion of IL into the pores. Finally, the sample was dried under high vacuum (2×10^{-3} mbar, room temperature) overnight in order to ensure complete removal of

DOI: 10.1021/am5074003
ACS Appl. Mater. Interfaces 2015, 7, 3562−3570

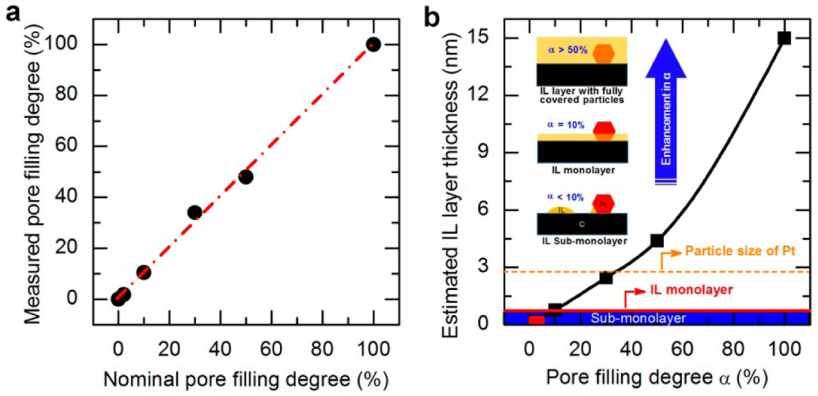

Figure 1. Pore filling degree α and IL layer thickness. (a) Comparison of the nominal pore filling degree with the measured one using N_2-sorption. (b) Estimation of IL layer thickness for SCILL systems at different pore filling degree. The inset gives the schematic illustration of the surface situation in the pores.

the solvent. Varying the IL amount in the isopropyl alcohol solution was used to adjust the pore filling degree.

Instrumentation. The water content of the IL was determined by Karl Fischer titration using a Metrohm 756 KF Coulometer with a Hydranal Coulomat AG reagent. The viscosity measurement was conducted at 25 °C using a MCR 100 rheometer Physica from Anton Paar. The viscosity given was averaged over the values obtained at shear rates in the range of 10−2000 s^{-1}. ^1H, ^{13}C and ^{19}F NMR spectra of the IL were recorded without further solvent using an insert tube filled with DMSO-d_6 on a Jeol ECX 400 spectrometer at 400, 100, and 376 MHz, respectively. Thermogravimetric analyses (TGA) were accomplished with a Setsys 1750 Cs Evolution (Setaram Instrumentation) thermogravimetric analyzer in nitrogen atmosphere at a heating rate of 10 °C min^{-1}, from room temperature to 900 °C. The porous property analysis was performed on Quantachrome Quadrasorb-SI Instrument using N_2-sorption at 77 K. Subsequent data evaluation was performed using QuadraWin software (Ver. 5.04). The surface area data of the samples were calculated by using the Brunauer−Emmett−Teller (BET) equation, while the total pore volume and micropore volume were determined by using the Barrett−Joyner−Halenda (BJH) and t-plot methods, respectively. The loading amount of Pt on the catalyst was determined by inductively coupled plasma atomic emission spectrometry (ICP-AES, PerkinElmer Plasma 400). The sample for ICP analysis was dissolved in a mixture of concentrated HF, HNO_3 and HCl solution in the proportion of 4:1:1. Transmission electron microscopy (TEM) images were captured using a Philips CM 300 UT microscope operated at 300 kV. The samples were prepared by placing a drop of catalyst powder dispersion in deionized water onto a carbon film coated copper grid (3 mm, 300 mesh), followed by drying under ambient conditions.

Electrochemical Measurements. Electrochemical measurements were carried out on a PARSTAT 4000 Potentiostat/Galvanostat (PAR) controlled by VersaStudio software. A leak-free double-junction Ag/AgCl electrode (Aldrich) and a Pt wire (PINE) were used as reference and counter electrodes, respectively. All potentials reported in this work were calibrated against reversible hydrogen electrode (RHE) using hydrogen evolution-oxidation reaction on a Pt electrode. A glassy carbon rotating disk electrode (GC-RDE, 5 mm diameter, PINE) was used as the working electrode. For rotating ring disk electrode (RRDE) measurement, a RRDE with glassy carbon as the disk electrode (diameter = 5.61 mm) and Pt as the ring electrode (PINE, collection efficiency N = 0.37) was used as the working electrode, and two PARSTAT 4000 potentiostats were used to control disk and ring potentials, respectively. Prior to each experiment, the GC-RDE was polished to a mirror finish using a 0.05 μm γ-alumina suspension (BUEHLER), followed by washing ultrasonically with ethanol, acetone and then deionized water to remove contaminants. To prepare the working electrode, a catalyst ink was prepared by sonicating a suspension of catalyst powder (5 mg) in a mixed solution of deionized water, isopropyl alcohol, 5% Nafion in the volume ratio of 4:1:0.025. For SCILL systems with α > 30%, a higher Nafion concentration (0.04 vol %) was used to aid dispersing the catalyst. A calibrated amount of catalyst ink for a 4 μg_{Pt} loading (i.e., 20.4 μg_{Pt} cm^{-2} based on the geometric area of the GC-RDE) was then pipetted onto the GC-RDE and dried under a gentle argon flow in order to form a uniform catalyst layer.

The electrochemical measurements were conducted at room temperature in N_2 or O_2 saturated 0.1 M $HClO_4$ solution. Before collecting the cyclic voltammetry (CV) curves for determination of electrochemically active surface area (EAS), the catalyst was first electrochemically cleaned via potential cycling between 0 and 1.3 V versus RHE for 20 cycles at 100 mV s^{-1}. The EAS was obtained by measuring the charges associated with the hydrogen desorption signals (Q_H) on the CV curves in N_2-saturated 0.1 M $HClO_4$, assuming 210 μC cm^{-2} for calibrating the desorption charge of a hydrogen monolayer on a Pt surface. The ORR measurements were performed in O_2-saturated 0.1 M $HClO_4$ electrolyte using GC-RDE at a rotation rate of 1600 rpm, and polarization curves were recorded at a scanning rate of 10 mV s^{-1}. Prior to each ORR measurement, the electrolyte was purged by bubbling with high purity oxygen for at least 30 min, and oxygen flow was then kept to avoid any disturbance from ambient atmosphere during the measurement. Furthermore, the IR-drop effect was compensated for all the ORR measurements, for which the solution resistance between the working and reference electrodes was determined by conducting AC impedance analysis (10 kHz, 5 mV). The coverage of OH_{ad} on Pt surface (θ_{OHad}) was calculated based on the OH_{ad} peak in the CV curves (0.6−0.9 V) and dividing the OH_{ad} area by the overall active surface area.

The mass-transport corrected kinetic current (i_k) used for assessment of ORR performance was calculated based on the Koutecky−Levich equation:

$$\frac{1}{i} = \frac{1}{i_{k,app}} + \frac{1}{i_d}$$

$$\frac{1}{i_{k,app}} = \frac{1}{i_k} + \frac{1}{i_p}$$

where i is the experimentally measured current from the positive going polarization curves, which have been corrected by subtracting background current (obtained in N_2-saturated electrolyte at a rotation rate of 1600 rpm); i_d is the diffusion limiting current; i_k is the kinetic current. To be noted, because only the outer diffusion and not the internal diffusion process of O_2 within the IL filled pores was considered in the Koutecky−Levich equation, not the intrinsic kinetic current but the apparent kinetic current ($i_{k,app}$) is obtained herein. The apparent kinetic current is not only determined on the intrinsic kinetics of ORR on Pt (i_k) but also on the internal diffusion of reactants within the porous system (i_p). The as-obtained apparent kinetic current was normalized to the EAS of Pt for every Pt/C-SCILL

DOI: 10.1021/am5074003
ACS Appl. Mater. Interfaces 2015, 7, 3562−3570

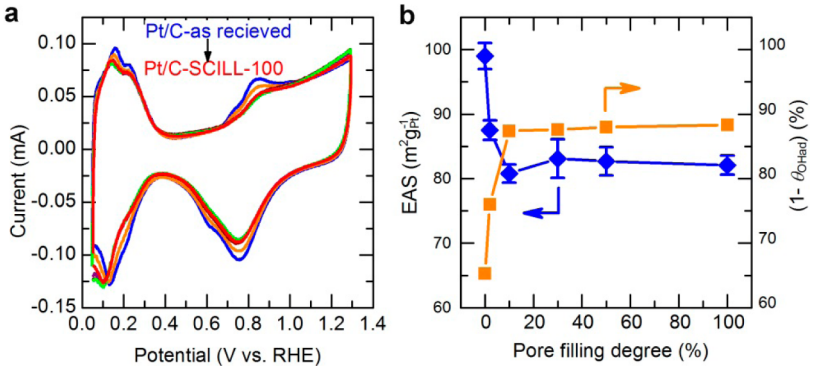

Figure 2. Electrochemical characterization. (a) Cyclic voltammetry curves of Pt/C-SCILL systems in N_2-saturated 0.1 M $HClO_4$ solution at a scanning rate of 20 mV s^{-1}. (b) EAS (blue) and free Pt sites ($1 - \theta_{OHad}$) @0.9 V (orange) as a function of the pore filling degrees for Pt/C-SCILL materials.

systems to obtain the apparent specific activity (SA_{app}) of Pt, which is still affected by internal mass transfer. At least three electrochemical experimental data sets were collected to generate the error bars, which were defined as the relative standard deviations for each measurement.

RESULTS AND DISCUSSION

Pt/C-SCILL samples were prepared by dispersing the commercial Pt/C catalyst (20 wt %, Johnson Matthey plc, UK) in an isopropyl alcohol solution containing the desired amount of [MTBD][NTf_2], followed by multistep solvent evaporation, as detailed in the Experimental Section. It is assumed that the IL is immobilized during the evaporation completely within the pore system due to its extremely low vapor pressure and the effective capillary forces. The set pore filling degree α was calculated based on the pore volume of the catalyst (1.22 mL g^{-1} from N_2-sorption) and the measured density of the IL (ρ_{IL}, 1.5 g cm^{-3}) with α being defined as

$$\alpha = \frac{V_{IL}}{V_{pore,0} \cdot m_{cat}}, \; V_{IL} = \frac{m_{IL}}{\rho_{IL}}$$

where m_{IL} and V_{IL} are the mass (g) and volume (mL) of the IL used in the preparation of SCILL systems, and m_{cat} and $V_{pore,0}$ are the mass (g) and specific pore volume (mL g^{-1}) of the Pt/C catalyst.

In this work, α was varied from 2 to 100% (named Pt/C-SCILL-XX with XX for α) and the resulting pore filling degree was analyzed by measuring the remaining specific pore volume with N_2-sorption (Figure S2, Supporting Information). We found that the measured α-values of the SCILL materials agree very well with the nominal values (Figure 1a). This indicates that the IL is immobilized completely; hence, avoiding loss of IL and allowing for a facile control of the pore filling degree of these SCILL systems during the preparation. It should also be noted that the pore volume of the applied Pt/C material is dominated by mesopores, with micropores possessing only a volume fraction of 1.5% on the fresh Pt/C material. This value reduced to 0.3% for SCILL-2 samples and below the detection limit for Pt/C-SCILL-10 and catalysts with higher IL loadings. Thus, flooding of the micropores is not critical and for the mesopores the formation of a large IL-water interface within the mesopores can be expected.[16]

Thermogravimetric analysis (TGA) was conducted to determine the mass loading and to probe the thermal stability of the SCILL materials. Figure S3 (Supporting Information) shows that fresh Pt/C catalyst has no significant weight loss up to 900 °C under N_2 atmosphere whereas [MTBD][NTf_2] is thermally stable up to 380 °C and leaves an ash content of 8 wt % after complete thermal decomposition. The IL supported on the Pt/C catalysts shows an earlier onset of decomposition than the neat IL at around 300 °C, which is still sufficiently high for the application in PEMFC. The lower decomposition temperature most likely originates from catalytic effects of the Pt nanoparticles[18] and also from the carbon−IL interaction, which is known to alter the decomposition pathway of [MTBD][NTf_2].[27,28] For SCILL-30 and SCILL-50, the weight loss up to 900 °C is estimated to be 34 and 44 wt %, respectively, considering the remaining ash content determined for the pure IL. These results corroborate the fact that Pt/C catalyst has been successfully coated with [MTBD][NTf_2]. However, the calculated weight loss values were slightly lower than the loading amount of IL (SCILL-30: 40.3 wt %; SCILL-50: 47.3 wt %). This is explained by alternative decomposition pathways in the presence of carbon and IL compared to the IL alone (with altered ash contents), e.g., induced by the strong hydrophobic interaction between IL and carbon materials.[18,29,30] The influence of the IL modification on the Pt nanoparticles was further studied using transmission electron microscopy (TEM). Representative images of the Pt/C and Pt/C-SCILL are shown in Figure S4 (Supporting Information). No significant change of the nanoparticle size (average 2.8 nm) and shape could be observed after IL impregnation.

The electrochemical properties of the as-prepared Pt/C-SCILL systems were studied and compared to the fresh reference Pt/C catalyst using the thin film rotating disk electrode technique. Figure 2a shows CV curves of Pt/C-SCILL systems recorded at room temperature in 0.1 M N_2-saturated $HClO_4$ solution. All catalysts show characteristic features of H adsorption/desorption on Pt in the potential region of 0.05 to 0.4 V and the formation of a surface oxidation (OH_{ad}) layer beyond 0.6 V. Compared to the reference Pt/C catalyst, the H adsorption/desorption peaks for the SCILL system are slightly suppressed, and the adsorption peak shifts toward lower potentials with increasing α-value. This is especially apparent when comparing the adsorption peaks for the samples with $\alpha < 10\%$. These data suggest that the presence of even a minor amount of IL suppresses the reductive adsorption of H on Pt, probably by reducing the Pt−H bonding strength through a ligand effect.[19,31]

The electrochemically active surface area (EAS) data, extracted from the hydrogen desorption peak (see the Experimental Section for detail) are compared in Figure 2b. The EAS for the Pt/C-fresh catalyst is determined to be 99.1

DOI: 10.1021/am5074003
ACS Appl. Mater. Interfaces 2015, 7, 3562−3570

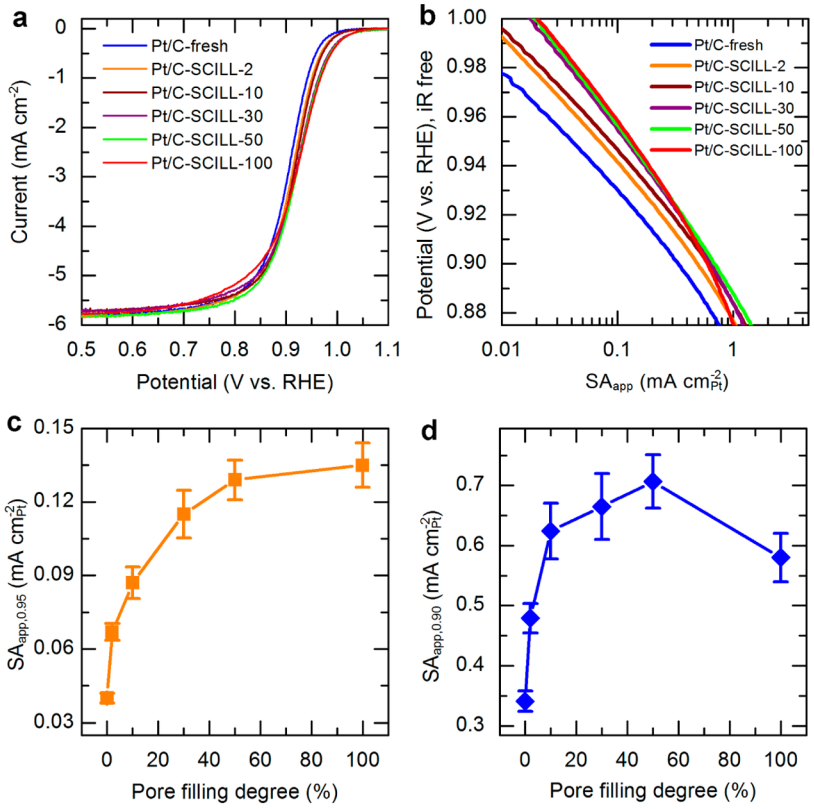

Figure 3. Oxygen reduction reaction on Pt/C and SCILL systems. (a) ORR polarization curves of Pt/C-SCILL systems compared to commercial Pt/C were recorded in O_2-saturated 0.1 M $HClO_4$ solution at a scanning rate of 10 mV s^{-1}. (b) ORR Tafel plots of Pt/C-SCILL systems extracted from the polarization curves in panel a. (c, d) Correlation between the apparent specific activity for ORR and the pore filling degree of the SCILL materials; the apparent specific activity data were compared at 0.95 (c) and 0.90 V (d), respectively.

$m^2\ g^{-1}_{Pt}$. Unexpectedly, introduction of a small amount of IL (α = 2%) into the Pt/C influences the EAS strongly, which reduces to 87.5 $m^2\ g^{-1}_{Pt}$. Increasing the IL content from α = 2% to 10% results in a further but less significant reduction in EAS from 87.5 to 80.8 $m^2\ g^{-1}_{Pt}$. Surprisingly, further addition of IL ($\alpha \geq$ 10%) does not affect the EAS (Figure 2b). The initial EAS loss may arise from the suppressed H adsorption on Pt through a ligand effect and/or the occupation of certain Pt sites by IL molecules preventing the adsorption of H atoms. Inspired by the work of Laurin et al., who found that imidazolium containing ILs (e.g., $[C_4C_1Im][NTf_2]$, for structure, see Scheme S2 in the Supporting Information) selectively replace CO molecules adsorbed on the (111) facets of Pt nanoparticles,[19] we estimated the surface fraction of (111) facets for a Pt nanoparticle with a size of 2.8 nm and cuboctahedral shape (see the Supporting Information). The resulting surface fraction of (111) facets (19.05%) coincided well with the maximum EAS loss (19.2%) of the SCILL systems. For Pt/C-SCILL-2, the lowest amount of IL was used for the modification, which resulted in the most pronounced EAS loss of 11.7%. Furthermore, for this catalyst the ratio of IL molecules to surface Pt atoms is 15.1%, which might indicate that the majority of the IL adsorbs onto the surface of Pt nanoparticles. Thus, the EAS drop could predominantly stem from the selective occupation of surface atoms by IL molecules.

Figure 2a,b also offers strong evidence that SCILL materials exhibit lower OH_{ad} coverage on Pt than fresh Pt/C, indicating that the IL in the SCILL system suppresses the surface oxidation of Pt nanoparticles. It is well accepted that too strong Pt−O bonding strength leads to a slow ORR kinetics on pure Pt.[2,32] Herein the suppression of Pt oxidation or the weakened Pt−O interaction on SCILL materials is expected to improve ORR kinetics by protecting the Pt sites from blocking by nonreactive oxygenated species.[2,32]

The electrocatalytic properties of the fresh Pt/C and the SCILL system for ORR were compared at room temperature in O_2-saturated 0.1 M $HClO_4$ solution. Polarization curves for ORR recorded in anodic direction are shown in Figure 3a. The diffusion limiting current is obtained in the potential region below 0.7 V for all the catalysts, followed by a mixed kinetic-diffusion control region between 0.8 and 1.0 V. Further inspection of Figure 3a reveals that the half-wave potentials ($E_{1/2}$) of the SCILL systems are always more positive than the reference fresh Pt/C catalyst (0.906 V), and increase monotonously with the pore filling degree. For instance, the $E_{1/2}$ value for Pt/C-SCILL-α is enhanced from 0.911 V at α = 2%, to 0.923 V at α = 30%, and 0.924 V for $\alpha \geq$ 50%. Since $E_{1/2}$ is an indicator of ORR overpotentials on these Pt catalysts, the positively shifted $E_{1/2}$ values suggest that the presence of IL in the SCILL systems accelerates the ORR kinetics on Pt. The high oxygen solubility of the IL and thus increased oxygen concentration at the active center is one possible reason for the increased activity.[26,27] Another major impact is seen in the increased number of free Pt sites available for the adsorption of O_2, which are generally believed to determine the ORR kinetics.[26,28,33] As demonstrated in Figure 2b, the coverage of Pt atoms by the nonreactive OH_{ad} species (θ_{OHad}) is substantially decreased on the SCILL system relative to the reference Pt/C. Hence, a higher number of free Pt sites (1 −

DOI: 10.1021/am5074003
ACS Appl. Mater. Interfaces 2015, 7, 3562−3570

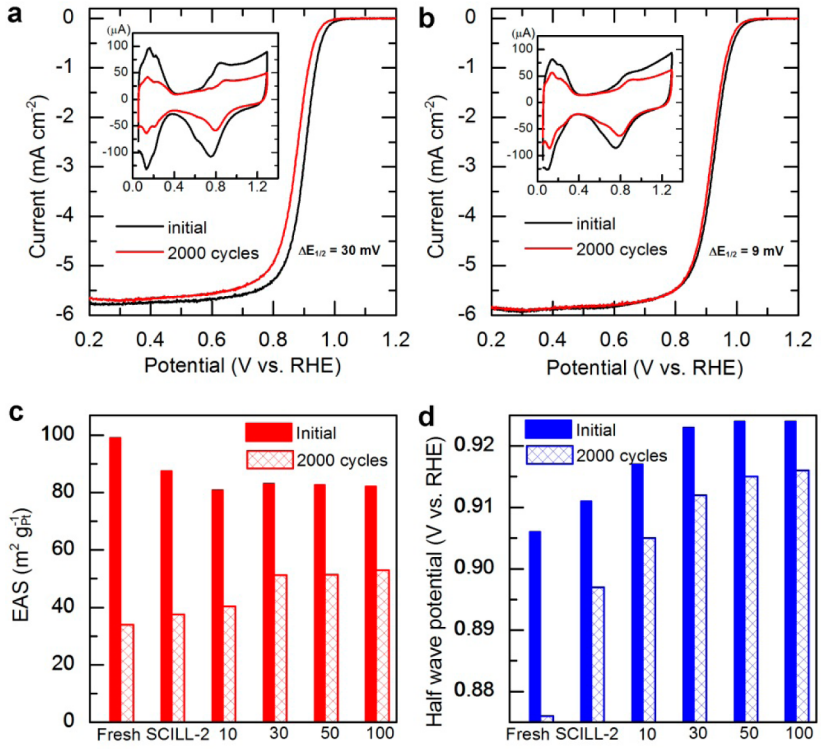

Figure 4. Durability measurements of reference Pt/C and SCILL systems. ORR polarization curves of Pt/C-fresh (a) and Pt/C-SCILL-50 (b) before and after 2000 potential cycles between 0.4 and 1.4 V in O_2-saturated 0.1 M $HClO_4$. The insets show the corresponding CV curves of each sample before and after the potential cycling. Summary of the electrochemically active surface area (c) and half-wave potential (d) of each sample before and after the durability test.

θ_{OHad}) available for the adsorption of O_2 will boost the activity strongly.

To elucidate whether the ionic liquid layer on these SCILL samples would affect oxygen reduction pathway or the H_2O_2 formation, the RRDE measurements were conducted on Pt/C-fresh and Pt/C-SCILL-50 samples in 0.1 M $HClO_4$ at a rotating rate of 1600 rpm, as displayed in Figure S5 (Supporting Information), whose upper panel plots the mole fraction of H_2O_2 formation versus potentials. It can be seen that the mole fraction of H_2O_2 formed during ORR is lower than 3% for both samples, indicating that the ORR is proceeding predominantly through the 4-electron transfer pathway on both samples. Besides, the comparable plots of fraction of H_2O_2 formation suggest that the tiny amount of ionic liquid indeed imposes little effect on the reaction mechanism of ORR on Pt surfaces

To quantitatively discuss the influence of the IL modification on the ORR activity, the apparent specific activity (SA_{app}) data were derived by normalizing the apparent kinetic current to the EAS of Pt, and compared in Figure 3b as a function of electrode potential. Comparisons of the SA_{app} data at 0.95 and 0.90 V are given in Figure 3c,d, respectively. It can be seen that these SA_{app} data strongly correlate with the pore filling degree of the SCILL systems. Specifically, the SA_{app} at 0.95 V ($SA_{app,0.95}$) increases with already 2% of pore filling from 0.04 to 0.07 mA cm^{-2}_{Pt}. Addition of further IL increases $SA_{app,0.95}$ to 0.13 mA cm^{-2}_{Pt} up to α = 50%, whereas further addition of IL shows no effect. On the basis of $SA_{app,0.95}$ data, Pt/C-SCILL-100 is 2 times more active than Pt/C-SCILL-2 and 3.4 times more active than the conventional Pt/C catalyst. These data can be partially rationalized by the higher amount of free sites ($1 - \theta_{OHad}$) on the SCILL system and the consequently accelerated ORR kinetics. However, this active-site coverage effect cannot explain the activity difference for all of the SCILL materials. For instance, although Pt/C-SCILL-10 and Pt/C-SCILL-100 possess similar θ_{OHad}, as illustrated in Figure 2a, the activity of the latter is almost 1.6 times higher than that of the former. Therefore, besides more abundant free Pt sites for O_2 adsorption on the SCILL systems, there must be other reasons for their enhanced ORR activity. Earlier work on ORR on Pt suggests that ORR kinetic current is dependent on the oxygen concentration at the Pt surface. Herein, the ionic liquid [MTBD][NTf_2] is reported to have O_2 solubility (2.28 mM)[11] nearly 2 times that of conventional $HClO_4$ electrolyte (1.21 mM).[11] The higher O_2 solubility of ionic liquids would increase the O_2 concentration at the Pt surface, resulting in higher attempt frequencies for the ORR and consequently higher activity.[26] It is assumed that with increasing the pore filling degree, Pt nanoparticles in the SCILL materials are covered to a higher amount by the IL film. This leads to more abundant surface Pt atoms, which are in direct contact with O_2-enriched IL layer. To better probe this process, the IL layer thickness in the pores was estimated (see the Supporting Information) and is plotted against the pore filling degree in Figure 1b. The resulting change in the IL-nanoparticle interaction is accordingly illustrated in the inset of Figure 1b. For the SCILL systems with α < 10%, the IL forms a submonolayer; with continuously increasing α, the IL layer gradually changes from a mono-ion pair layer ($\alpha \approx$ 10%) to multilayers (α > 10%). For the observed average Pt particle size of 2.8 nm the active metal clusters would be fully covered above 50% IL pore filling. Consistently, the $SA_{app,0.95}$ data of these SCILL systems increase initially with α, leveling off at α > 50%.

When the SA_{app} data at 0.90 V ($SA_{app,0.90}$) are compared, a potential where diffusion-limitation becomes more predom-

DOI: 10.1021/am5074003
ACS Appl. Mater. Interfaces 2015, 7, 3562−3570

inant, a volcano dependence of $SA_{app,0.90}$ on α-value and maximum $SA_{app,0.90}$ at α = 50% is found (Figure 3d). To rationalize this phenomenon, we need to revisit the effect of the IL layer in the SCILL system. As mentioned above, the high O_2 solubility of IL increases the O_2 mass transport to the catalytic surface. Moreover, the IL increases the number of free sites, further facilitating the ORR kinetics on the SCILL system. However, at relatively high overpotentials, the diffusion rate of O_2 molecules to the catalytic surface plays a more important role in controlling the reaction rate, which could be the reason for the drop in apparent activity above 50% of pore filling. The diffusion coefficient of O_2 in [MTBD][NTf_2] can be estimated using the Stokes−Einstein equation and IL-viscosity at 298 K (122 cP, see Figure S6 in the Supporting Information for details).[34,35] The result indicates that O_2 diffusion coefficient in [MTBD][NTf_2] (1.5×10^{-7} cm^2 s^{-1}) is almost 2 orders of magnitude lower than that in 0.1 M $HClO_4$ (1.9×10^{-5} cm^2 s^{-1}).[36] Thus, the diffusion within the IL can show a pronounced influence on the apparent kinetics. For lower IL fillings the pores still contain a significant share of aqueous electrolyte that promotes the mass transfer of O_2.

Summarizing, for the SCILL systems with a low α-value, ORR kinetics are increasing due to reduced OH adsorption and resulting higher amount of free active sites, and partially due to higher O_2 concentration where the IL wets the active sites. Nevertheless, while the Pt nanoparticles are not fully covered by IL, a certain percentage of surface Pt atoms cannot directly contact the O_2-enriched IL layer and thus ORR kinetics is not fully boosted. On the contrary, for SCILL systems with a too high an α-value, long diffusion pathways in completely IL flooded pores restrict the diffusion of O_2 from bulk electrolyte to catalytic surfaces, leading to a low effective O_2 concentration at the catalyst and resulting in a lower ORR reaction rate. Therefore, both the positive and negative consequences of IL contribute to the observed volcano-shaped dependence of ORR rate on the α-value. These results also indicate that an optimal configuration to achieve higher catalytic activity for ORR combines fully covered platinum particles with not fully flooded pores, where the remaining electrolyte channels allow for fast O_2 mass transport. For the precious Pt catalyst, high mass activity is more essential in view of practical applications. Notably, the SCILL-50 possesses a high mass activity of 0.56 A mg^{-1}_{Pt} at 0.9 V, which is above the mass activity target (0.44 A mg^{-1}_{Pt} @0.9 V) set by US Department of Energy for 2017−2020 demonstrating the potential of the SCILL approach for Pt-based electrocatalysis.

The durability of the catalysts was also evaluated by potential cycling between 0.4 and 1.4 V for 2000 cycles in an O_2-saturated 0.1 M $HClO_4$ solution (1 V s^{-1}, room temperature). It should be noted that equal amounts of Pt on the RDE (20 $\mu g \cdot cm^{-2}$) were used for the durability test on all the catalysts. This was to enable a fair comparison in consideration of the fact that the loading amount of Pt on the electrode can have a significant influence on the catalyst stability in this test.[37] Figure 4 shows the polarization curves and voltammograms of the reference Pt/C and the Pt/C-SCILL-50 system before and after the potential cycling. After 2000 cycles, the reference Pt/C catalyst showed a degradation of 30 mV in terms of half-wave potential (Figure 4a). Surprisingly, the degradation of the Pt/C-SCILL is much less significant, with only 9 mV negative shift in half-wave potential (Figure 4b). This indicates an additional advantage of the Pt/C-SCILL electrocatalysis system with respect to durability and stability. It is noteworthy that after cycling the Pt/C-SCILL-50 system it still shows a higher half-wave potential compared to the fresh reference Pt/C catalyst. Although with neat Pt/C, only 34% of the original Pt EAS remained after the potential cycling (inset in Figure 4a), the Pt/C-SCILL-50 system preserved 62% of its initial EAS (inset in Figure 4b). Figure 4c,d summarizes the electrochemical properties of the SCILL system and Pt/C reference before and after the potential cycling, while the activity data were summarized in Table S2 (Supporting Information). It can be observed that all the samples exhibit comparable SA_{app} before and after the stability test, while significant loss in mass activity was also detected on all the samples, which could arise from the drop in the active surface area. The SCILL materials exhibit superior durability performance. The stability increases in terms of both EAS and half-wave potential drops with higher α-value and settles approximately at 30% pore filling. The improved stability of the SCILL materials may partially arise from the suppressed surface oxidation of Pt nanoparticles encapsulated by IL. To better understand the degradation behavior, TEM characterization was performed after the stability test (Figure S7, Supporting Information). A number of particle aggregations with irregular shapes can be observed on Pt/C-fresh after 2000 potential cycles, with the average size enlarged from 2.8 nm on initial sample to 5.5 nm. In contrast, the Pt nanoparticles are more evenly distributed on Pt/C-SCILL-50 after stability test, though average particle size enlargement from 2.8 to 4.4 nm was also observed. This result indicates that the IL layer with wide electrochemical window and chemical stability providing a steric and electrostatic protection against agglomeration of Pt nanoparticles would play a key role in improving the stability of the SCILL materials.[38] For the unmodified Pt/C a drop in double layer charging current is also observed after the durability test, while this is not the case for Pt/C-SCILL-50 system, for which the CV curves at double layer region (0.35−0.45 V) are well overlapped. This indicates that carbon corrosion, which is also a major cause of cathode catalyst degradation, is suppressed on the SCILL system.

CONCLUSION

This work provides evidence that Pt/C electrocatalysts for ORR can greatly benefit from surface modification with hydrophobic, fluorinated ionic liquids. The preparation method is simple and highly suitable for scale-up. The influence of different pore filling degrees has been studied in detail. For an optimal SCILL system for ORR, the IL loading has been found to be 50 vol % of the support's pore volume. Thus, the advantages of increased number of free sites (lowered OH_{ad} coverage) and increased O_2 availability at the catalyst surface with still sufficient O_2 mass transfer through the aqueous phase into the pores of the catalyst system can be fully exploited. We could show that such optimized SCILL systems were more active and more stable in the ORR compared to an unmodified commercial Pt/C catalyst. Thus, we anticipate that these systems are highly promising for future fuel cell applications.

ASSOCIATED CONTENT

Supporting Information

Estimation of IL thickness, determination of Pt(111) surface fractions, calculation of the diffusion coefficient of O_2 in IL, IL structures, N_2 sorption, TG analysis, TEM characterizations, RRDE measurements, viscosity flow curves, NMR of IL and activity data before and after stability test. This material is available free of charge via the Internet at http://pubs.acs.org.

DOI: 10.1021/am5074003
ACS Appl. Mater. Interfaces 2015, 7, 3562−3570

AUTHOR INFORMATION

Corresponding Author

*Prof. Bastian J. M. Etzold. Tel.: +49 (9131) 85-27430. Fax: +49 (9131) 85-27421. E-mail: bastian.etzold@fau.de.

Notes

The authors declare no competing financial interest.

ACKNOWLEDGMENTS

The authors gratefully acknowledge the funding of the German Research Council (DFG), which, within the framework of its Excellence Initiative, supports the Cluster of Excellence "Engineering of Advanced Materials" (www.eam.uni-erlangen.de) at the University of Erlangen-Nürnberg. We acknowledge Dr. Nicola Taccardi (Lehrstuhl für Chemische Reaktionstechnik) for his kind help in the synthesis of ionic liquid, Dr. Marco Haumann and Prof. Peter Wasserscheid for the fruitful scientific discussions and Prof. Robin Klupp Taylor for his comments on the paper.

REFERENCES

(1) Zhang, J.; Sasaki, K.; Sutter, E.; Adzic, R. R. Stabilization of Platinum Oxygen-Reduction Electrocatalysts Using Gold Clusters. *Science* **2007**, *315*, 220−222.

(2) Stamenkovic, V. R.; Fowler, B.; Mun, B. S.; Wang, G. F.; Ross, P. N.; Lucas, C. A.; Markovic, N. M. Improved Oxygen Reduction Activity on $Pt_3Ni(111)$ via Increased Surface Site Availability. *Science* **2007**, *315*, 493−497.

(3) Debe, M. K. Electrocatalyst Approaches and Challenges for Automotive Fuel Cells. *Nature* **2012**, *486*, 43−51.

(4) Lim, B.; Jiang, M. J.; Camargo, P. H. C.; Cho, E. C.; Tao, J.; Lu, X. M.; Zhu, Y. M.; Xia, Y. N. Pd-Pt Bimetallic Nanodendrites with High Activity for Oxygen Reduction. *Science* **2009**, *324*, 1302−1305.

(5) Feng, Y. Y.; Zhang, G. R.; Ma, J. H.; Liu, G.; Xu, B. Q. Carbon-Supported Pt^Ag Nanostructures as Cathode Catalysts for Oxygen Reduction Reaction. *Phys. Chem. Chem. Phys.* **2011**, *13*, 3863−3872.

(6) Shao, Y. Y.; Yin, G. P.; Gao, Y. Z. Understanding and Approaches for the Durability Issues of Pt-based Catalysts for PEM Fuel Cell. *J. Power Sources* **2007**, *171*, 558−566.

(7) Zhang, J.; Lima, F. H. B.; Shao, M. H.; Sasaki, K.; Wang, J. X.; Hanson, J.; Adzic, R. R. Platinum Monolayer on Nonnoble Metal-Noble Metal Core-Shell Nanoparticle Electrocatalysts for O_2 Reduction. *J. Phys. Chem. B* **2005**, *109*, 22701−22704.

(8) Wang, C.; van der Vliet, D.; More, K. L.; Zaluzec, N. J.; Peng, S.; Sun, S. H.; Daimon, H.; Wang, G. F.; Greeley, J.; Pearson, J.; Paulikas, A. P.; Karapetrov, G.; Strmcnik, D.; Markovic, N. M.; Stamenkovic, V. R. Multimetallic Au/$FePt_3$ Nanoparticles as Highly Durable Electrocatalyst. *Nano Lett.* **2011**, *11*, 919−926.

(9) Guo, S. J.; Li, D. G.; Zhu, H. Y.; Zhang, S.; Markovic, N. M.; Stamenkovic, V. R.; Sun, S. H. FePt and CoPt Nanowires as Efficient Catalysts for the Oxygen Reduction Reaction. *Angew. Chem., Int. Ed.* **2013**, *52*, 3465−3468.

(10) Stamenkovic, V. R.; Mun, B. S.; Arenz, M.; Mayrhofer, K. J. J.; Lucas, C. A.; Wang, G. F.; Ross, P. N.; Markovic, N. M. Trends in Electrocatalysis on Extended and Nanoscale Pt-Bimetallic Alloy Surfaces. *Nat. Mater.* **2007**, *6*, 241−247.

(11) Chen, C.; Kang, Y. J.; Huo, Z. Y.; Zhu, Z. W.; Huang, W. Y.; Xin, H. L. L.; Snyder, J. D.; Li, D. G.; Herron, J. A.; Mavrikakis, M.; Chi, M. F.; More, K. L.; Li, Y. D.; Markovic, N. M.; Somorjai, G. A.; Yang, P. D.; Stamenkovic, V. R. Highly Crystalline Multimetallic Nanoframes with Three-Dimensional Electrocatalytic Surfaces. *Science* **2014**, *343*, 1339−1343.

(12) Colon-Mercado, H. R.; Kim, H.; Popov, B. N. Durability Study of Pt_3Ni_1 Catalysts as Cathode in PEM Fuel Cells. *Electrochem. Commun.* **2004**, *6*, 795−799.

(13) Jinnouchi, R.; Anderson, A. B. Electronic Structure Calculations of Liquid-Solid Interfaces: Combination of Density Functional Theory and Modified Poisson-Boltzmann Theory. *Phys. Rev. B* **2008**, *77*, 245417.

(14) Yeh, K. Y.; Wasileski, S. A.; Janik, M. J. Electronic Structure Models of Oxygen Adsorption at the Solvated, Electrified Pt(111) Interface. *Phys. Chem. Chem. Phys.* **2009**, *11*, 10108−10117.

(15) Bondarenko, A. S.; Stephens, I. E. L.; Hansen, H. A.; Perez-Alonso, F. J.; Tripkovic, V.; Johansson, T. P.; Rossmeisl, J.; Norskov, J. K.; Chorkendorff, I. The Pt(111)/Electrolyte Interface under Oxygen Reduction Reaction Conditions: An Electrochemical Impedance Spectroscopy Study. *Langmuir* **2011**, *27*, 2058−2066.

(16) Kernchen, U.; Etzold, B.; Korth, W.; Jess, A. Solid Catalyst with Ionic Liquid Layer (SCILL) - A New Concept to Improve Selectivity Illustrated by Hydrogenation of Cyclooctadiene. *Chem. Eng. Technol.* **2007**, *30*, 985−994.

(17) Arras, J.; Steffan, M.; Shayeghi, Y.; Ruppert, D.; Claus, P. Regioselective Catalytic Hydrogenation of Citral with Ionic Liquids as Reaction Modifiers. *Green Chem.* **2009**, *11*, 716−723.

(18) Lemus, J.; Palomar, J.; Gilarranz, M. A.; Rodriguez, J. J. Characterization of Supported Ionic Liquid Phase (SILP) Materials Prepared from Different Supports. *Adsorption* **2011**, *17*, 561−571.

(19) Sobota, M.; Happel, M.; Amende, M.; Paape, N.; Wasserscheid, P.; Laurin, M.; Libuda, J. Ligand Effects in SCILL Model Systems: Site-Specific Interactions with Pt and Pd Nanoparticles. *Adv. Mater.* **2011**, *23*, 2617−2621.

(20) Steinruck, H. P.; Libuda, J.; Wasserscheid, P.; Cremer, T.; Kolbeck, C.; Laurin, M.; Maier, F.; Sobota, M.; Schulz, P. S.; Stark, M. Surface Science and Model Catalysis with Ionic Liquid-Modified Materials. *Adv. Mater.* **2011**, *23*, 2571−2587.

(21) Buzzeo, M. C.; Evans, R. G.; Compton, R. G. Non-Haloaluminate Room-Temperature Ionic Liquids in Electrochemistry - A Review. *ChemPhysChem* **2004**, *5*, 1106−1120.

(22) Liu, H. T.; Liu, Y.; Li, J. H. Ionic Liquids in Surface Electrochemistry. *Phys. Chem. Chem. Phys.* **2010**, *12*, 1685−1697.

(23) Parvulescu, V. I.; Hardacre, C. Catalysis in Ionic Liquids. *Chem. Rev.* **2007**, *107*, 2615−2665.

(24) Svancara, I.; Vytras, K.; Kalcher, K.; Walcarius, A.; Wang, J. Carbon Paste Electrodes in Facts, Numbers, and Notes: A Review on the Occasion of the 50-Years Jubilee of Carbon Paste in Electrochemistry and Electroanalysis. *Electroanalysis* **2009**, *21*, 7−28.

(25) Hapiot, P.; Lagrost, C. Electrochemical Reactivity in Room-Temperature Ionic Liquids. *Chem. Rev.* **2008**, *108*, 2238−2264.

(26) Snyder, J.; Fujita, T.; Chen, M. W.; Erlebacher, J. Oxygen Reduction in Nanoporous Metal-Ionic Liquid Composite Electrocatalysts. *Nat. Mater.* **2010**, *9*, 904−907.

(27) Snyder, J.; Livi, K.; Erlebacher, J. Oxygen Reduction Reaction Performance of [MTBD][beti]-Encapsulated Nanoporous NiPt Alloy Nanoparticles. *Adv. Funct. Mater.* **2013**, *23*, 5494−5501.

(28) Tan, Y. M.; Xu, C. F.; Chen, G. X.; Zheng, N. F.; Xie, Q. J. A Graphene-Platinum Nanoparticles-Ionic Liquid Composite Catalyst for Methanol-Tolerant Oxygen Reduction Reaction. *Energy Environ. Sci.* **2012**, *5*, 6923−6927.

(29) Shul, G.; Sirieix-Plenet, J.; Gaillon, L.; Opallo, M. Ion Transfer at Carbon Paste Electrode Based on Ionic Liquid. *Electrochem. Commun.* **2006**, *8*, 1111−1114.

(30) Sun, W.; Yang, M. X.; Li, Y. Z.; Jiang, Q.; Liu, S. F.; Jiao, K. Electrochemical Behavior and Determination of Rutin on A Pyridinium-based Ionic Liquid Modified Carbon Paste Electrode. *J. Pharm. Biomed. Anal.* **2008**, *48*, 1326−1331.

(31) Arras, J.; Paki, E.; Roth, C.; Radnik, J.; Lucas, M.; Claus, P. How a Supported Metal Is Influenced by an Ionic Liquid: In-Depth Characterization of SCILL-Type Palladium Catalysts and Their Hydrogen Adsorption. *J. Phys. Chem. C* **2010**, *114*, 10520−10526.

(32) Stamenkovic, V.; Mun, B. S.; Mayrhofer, K. J. J.; Ross, P. N.; Markovic, N. M.; Rossmeisl, J.; Greeley, J.; Norskov, J. K. Changing the Activity of Electrocatalysts for Oxygen Reduction by Tuning the Surface Electronic Structure. *Angew. Chem., Int. Ed.* **2006**, *45*, 2897−2901.

DOI: 10.1021/am5074003
ACS Appl. Mater. Interfaces 2015, 7, 3562−3570

(33) Gomez-Marin, A. M.; Rizo, R.; Feliu, J. M. Some Reflections on the Understanding of the Oxygen Reduction Reaction at Pt(111). *Beilstein J. Nanotechnol.* **2013**, *4*, 956−967.
(34) Khan, A.; Lu, X. Y.; Aldous, L.; Zhao, C. Oxygen Reduction Reaction in Room Temperature Protic Ionic Liquids. *J. Phys. Chem. C* **2013**, *117*, 18334−18342.
(35) Lu, Y. C.; Kwabi, D. G.; Yao, K. P. C.; Harding, J. R.; Zhou, J. G.; Zuin, L.; Shao-Horn, Y. The Discharge Rate Capability of Rechargeable Li-O_2 Batteries. *Energy Environ. Sci.* **2011**, *4*, 2999−3007.
(36) Wei, Y. C.; Liu, C. W.; Wang, K. W. Improvement of Oxygen Reduction Reaction and Methanol Tolerance Characteristics for PdCo Electrocatalysts by Au Alloying and CO Treatment. *Chem. Commun.* **2011**, *47*, 11927−11929.
(37) Meier, J. C.; Galeano, C.; Katsounaros, I.; Witte, J.; Bongard, H. J.; Topalov, A. A.; Baldizzone, C.; Mezzavilla, S.; Schuth, F.; Mayrhofer, K. J. J. Design Criteria for Stable Pt/C Fuel Cell Catalysts. *Beilstein J. Nanotechnol.* **2014**, *5*, 44−67.
(38) Favier, I.; Madec, D.; Gómez, M. *Metallic Nanoparticles in Ionic Liquids − Applications in Catalysis*, 1st ed; Wiley-VCH Verlag & Co. KGaA: Weinheim, Germany, 2013.

DOI: 10.1021/am5074003
ACS Appl. Mater. Interfaces 2015, 7, 3562−3570